Acoustic damping of an annular tail-pipe under mean flow conditions

Rene Boonen, Paul Sas
Department of Mechanical Engineering, P.M.A., KULeuven, Celestijnenlaan 300 B, B-3001, Heverlee, Belgium.

Eric Van den Bulck
Department of Mechanical Engineering, T.M.E., KULeuven, Celestijnenlaan 300 B, B-3001, Heverlee, Belgium.

Summary
A damping device, consisting of an annular tail-pipe, has been developed. It is applicable in situations wherein acoustic damping is required in combination with low flow resistance. The device consists of a central tube surrounded by a narrow slit. The central tube has an acoustic mass which impedance increases with frequency while the slit resistance remains constant. When the frequency has been increased sufficiently, a considerable part of the acoustic flow passes through the slit where it will be damped. In this way, acoustic energy can be dissipated while the flow experiences a low flow resistance. The acoustic properties of the device will be investigated using an electrical equivalent circuit. The impedance will be measured using an impedance measurement duct, from which the slit resistance will be deduced. The resulting slit resistance consists of a linear part depending on the air viscosity, and a non-linear part which is caused by the loss of kinetic energy of the fluidum through the slit. The presence of a laminar mean flow does not effect the acoustic performance of the annular tailpipe, only some minor effects are observed in the low frequency range. Even with a mean turbulent flow, the acoustic damping mechanism still remains intact.

PACS no. 43.25.Ed, 43.50.Gf, 47.15.Rq

1. Introduction

Several applications require high acoustic damping in combination with low flow resistance. These applications concern for example gas flow machines such as ventilation systems, turbo-engines, intake and exhaust systems for internal combustion engines. In several cases, absorption is realized by placing resistive materials in the flow, such as fibre materials, foams, perforated plates or metal weaving. They are quite efficient to suppress noise, however they can generate a considerable pressure drop.

In this paper, a damping device will be presented, consisting of a central tube with negligible flow resistance surrounded by a narrow slit to generate the acoustic damping. The central tube behaves as an acoustic mass which impedance is proportional to frequency. The slit acts as a resistance and remains approximately constant in terms of frequency. When the frequency has been increased sufficiently, a considerable part of the acoustic flow passes through the slit where it will be damped. In this way, acoustic energy can be dissipated while the flow experiences a low flow resistance.

A measurement setup has been developed, consisting of an impedance duct with an annular tail pipe at the end. The acoustic damping capability of the device will be investigated in two phases. First, the impedance of the damping device will be measured without mean flow using the two microphone transfer function method according to ISO 10534-2 on an improved measurement wave guide [1]. An electrical equivalent model has been used to validate the measurement results and to extract the resistance of the slit from the measurements. A non-linear analysis has been performed to investigate the slit resistance in terms of frequency and acoustic excitation level. Second, a mean flow is superposed on the acoustic excitation. The impedance measurements will be corrected for the mean flow [2]. The effects on the mean flow on the acoustic damping will be presented. Ultimately, it will appear that the effects of a laminar flow on the acoustic damping of the device will be negligible. With turbulent flow, the acoustical resistance of the slit decreases in the low frequency range.

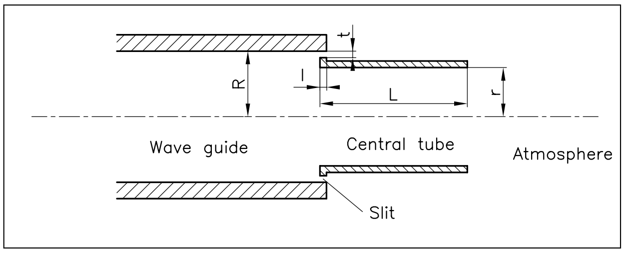

Figure 1. Scheme of the damping device.

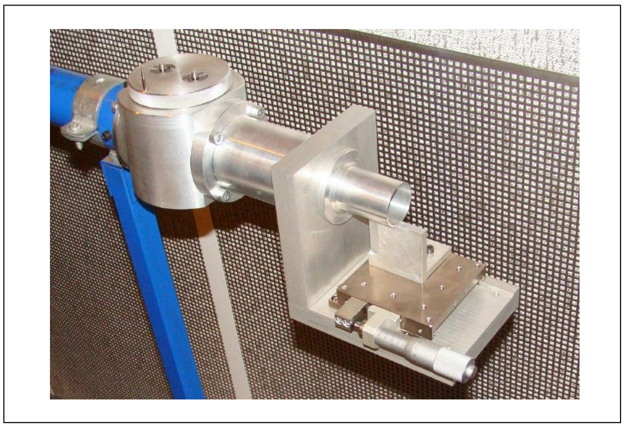

Figure 2. Photo of the damping device.

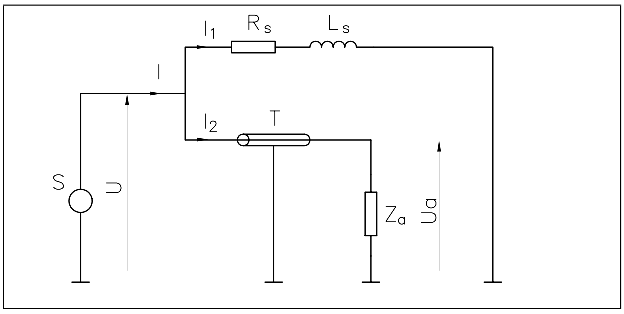

Figure 3. Electrical equivalent circuit of the damping device.

2. Configuration of the damping device

The construction of the damping device is presented in figure 1. A photograph of the device is presented in figure 2. At the left side situates the wave guide through which the waves are incoming. The wave guide consist of a duct with radius $R = 20\,\mathrm{mm}$. The damping device consists of a central tube with length $L = 45\,\mathrm{mm}$ and radius $r = 15\,\mathrm{mm}$. Between the central tube and the wave guide wall, the narrow slit is situated. The slit has a length $l = 1.5\,\mathrm{mm}$ and is $t = 0.2\,\mathrm{mm}$ wide. Both the central tube and the slit are connected to the atmosphere at the right side.

The analysis of the damping device is carried out using an equivalent electrical circuit, which is presented in figure 3. The voltage U represents the pressure p at the left side of the central tube in figure 1. The current I represents the acoustic flow Φ which divides in a current I_1 through the slit and I_2 through the central tube. The slit is represented by its resistance R_s and its acoustic mass L_s. The central tube is represented by the wave guide T with characteristic impedance $Z_c = \frac{\rho\, c}{\pi\, r^2}$ and is closed by the spherical radiator Z_a, representing the atmosphere.

In order to determine the acoustic dissipation in the slit, the currents in the two branches in the circuit have to be determined. Therefore, the impedance of each branch has be determined. The impedance of the branch containing the central tube is determined from the transfer matrices:

$$\begin{bmatrix} U \\ I_2 \end{bmatrix} = \begin{bmatrix} \cos k\,L & j\,Z_c\,\sin k\,L \\ \dfrac{j}{Z_c}\,\sin k\,L & \cos k\,L \end{bmatrix} \begin{bmatrix} 1 & 0 \\ \dfrac{1}{Z_a} & 1 \end{bmatrix} \begin{bmatrix} U_a \\ 0 \end{bmatrix} \quad (1)$$

wherein k is the wave number, $j = \sqrt{-1}$, L the length of the central tube, Z_c the characteristic impedance of the central tube and $Z_a = \frac{\rho\, c}{\pi\, r^2}\, \frac{j\, k\, r}{1 + j\, k\, r}$ the spherical radiator impedance representing the atmosphere. ρ is the air density, c the speed of sound and r the central tube radius. The impedance of the central tube Z_2 results then from equation (1):

$$Z_2 = \frac{U}{I_2} = \frac{\cos k\,L + j\,\dfrac{Z_c}{Z_a}\,\sin k\,L}{\dfrac{j}{Z_c}\,\sin k\,L + \dfrac{1}{Z_a}\,\cos k\,L} \quad (2)$$

The impedance Z_1 of the upper branch containing the slit will be:

$$Z_1 = R_s + j\,\omega\,L_s \quad (3)$$

with $\omega = 2\,\pi\,f = \frac{k}{c}$ the angle frequency, R_s the slit resistance and $L_s = \frac{\rho\, l}{2\,\pi\, R\, t}$ the acoustical mass of the slit, with $2\,\pi\,R$ the slit circumference and t the slit width. The total impedance of the device will be

$$Z = \frac{Z_1\,Z_2}{Z_1 + Z_2} \quad (4)$$

which will be measured using the two microphone transfer function method from which the slit resistance R_s will be determined.

3. Impedance and particle velocity measurement method

In the case of still-standing medium, the impedance Z of the device will be measured using the two microphone transfer function method according to the standard ISO 10534-2 [3]. The particle velocity u at the reference section will be calculated from the linear spectra measured at the two microphone locations using Euler's law:

$$\frac{\Delta p}{\Delta x} = -\rho\,j\,\omega\,u_c \quad (5)$$

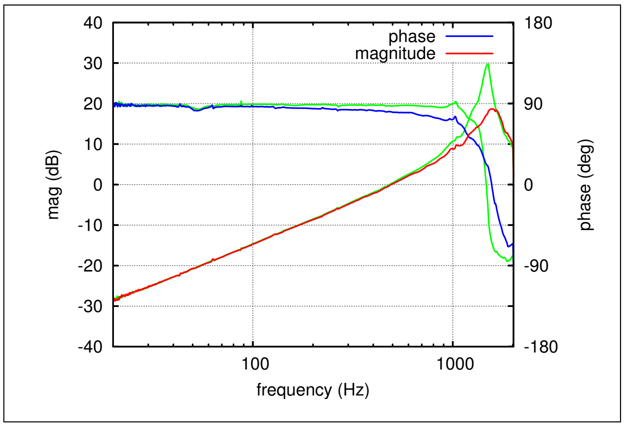

Figure 4. Comparison of the impedance of the device with open slit in magnitude (red line),(reference 0dB= Z_0) and phase (blue line) and the impedance with closed slit (green line).

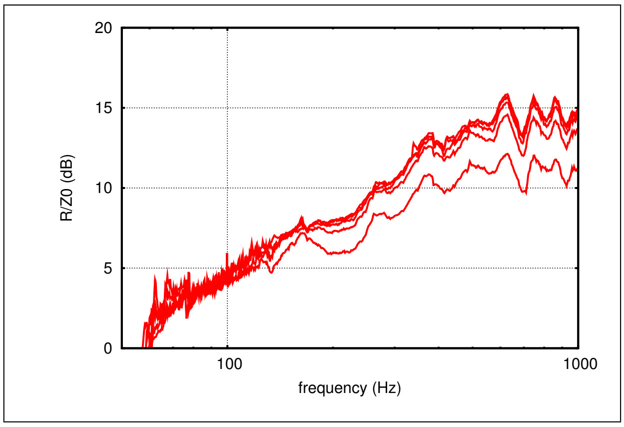

Figure 5. Magnitude of the slit resistance in terms of frequency for different loudspeaker excitation levels. Lowest curve: 10V, curve above 20V and so on for 30V, 60V to the upper curve 100V.

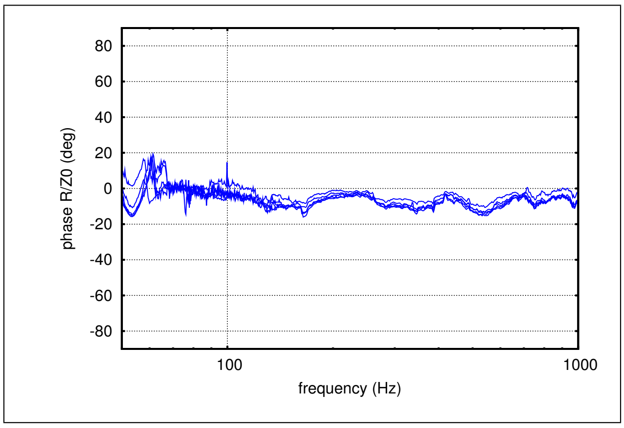

Figure 6. Phase of the slit resistance in terms of frequency for different loudspeaker excitation levels.

wherein Δp is the pressure difference between the microphones, Δx the distance between the microphones and u_c the particle velocity in the center between the microphones. The particle velocity $u = \frac{\Phi}{\pi R^2}$ at the reference section will then be determined from the particle velocity u_c:

$$u = u_c \frac{1 - \Gamma}{e^{j\,\omega\,(x_1+x_2)/(2\,c)} - \Gamma\, e^{-j\,\omega\,(x_1+x_2)/(2\,c)}} \qquad (6)$$

in which Γ is the reflection coefficient to the damping device, determined from its impedance Z and the characteristic impedance of the measurement duct Z_0. For moving medium, the expressions for the acoustic wave number k and the duct's characteristic impedance Z_0 are adapted using the Mach number as proposed by Munjal [2].

4. Measurement results

The measurements are carried out on the impedance duct using a dynamic signal analyser SRS785 with two PCB106B microphones. A 60W loudspeaker is excited using different voltages i.e. 10V, 20V, 30V, 60V and 100V to vary the particle velocity at the device. For each voltage, the transfer functions between the two microphones and the linear pressure spectra at each microphone have been measured to determine the impedance Z and the particle velocity u. Then, from expression (4), the resistance R_s of the slit will be determined and its dependence in terms of frequency and particle velocity will be investigated.

In first instance, the measurements are carried out in still-standing medium. Figure 4 presents the measured device impedance Z in magnitude (red line) and phase (blue line) when 60 V has been applied on the loudspeaker. The measured impedance of the closed slit has been plotted over it (green line). The phase delay between the closed and open slit impedance indicates a considerable effect of the slit resistance on the total impedance.

The slit resistance, obtained from the measured impedance, is presented in figure 5 in magnitude (reference 0 dB= Z_0) and in figure 6 in phase for all applied voltages to the loudspeaker. The resistance magnitude increases with the loudspeaker level, i.e. the lowest curve is measured using 10 V, the curve above with 20 V, then 30 V, 60 V until the upper curve with 100 V. The phase of the slit resistance, presented in figure 6, situates for all loudspeaker levels around the zero degrees, which confirms the resistive nature of the slit. The phase curves do not follow the sequence of the loudspeaker levels such as the resistance magnitudes do.

The real part of the slit resistance (thick red lines) in terms of the particle velocity through the slit is presented in figure 7 for different frequencies. Each curve consists of five points and exhibits a linear relationship between the slit resistance and the particle velocity through it. There is no definite sequence of the curves in terms of frequency, which suggests that

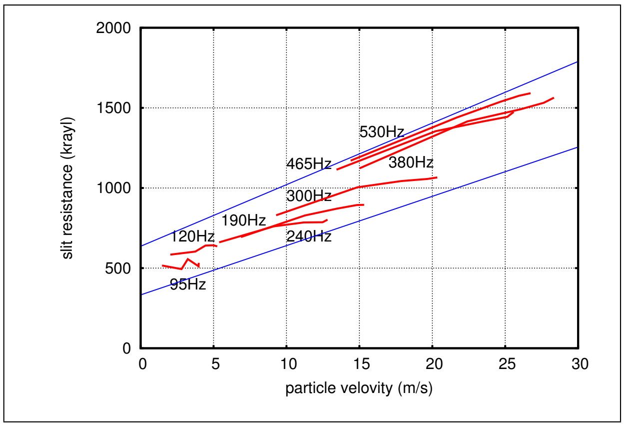

Figure 7. Slit resistance in terms of particle velocity through the slit for different frequencies (thick red lines: measured, thin blue lines: simulated using expression (18))

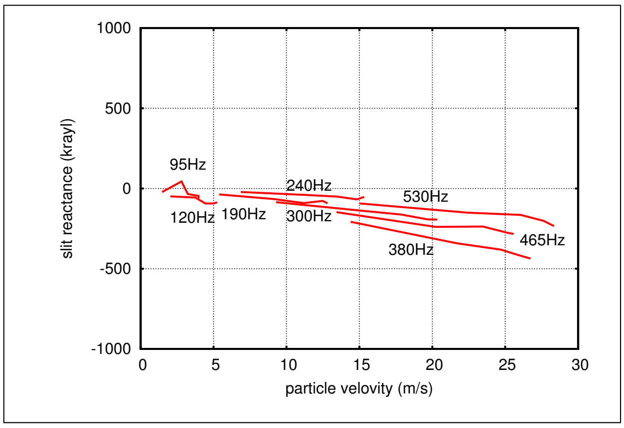

Figure 8. Measured slit reactance in terms of particle velocity through the slit for different frequencies.

there is no relation between the slit resistance and frequency. The imaginary part of the slit impedance, wherein the acoustic mass of the slit is included, is presented in figure 8. The reactance magnitude is considerably smaller than the resistance.

5. Analysis of the slit resistance

The slit resistance can be considered as the sum of a linear part (constant resistance) and a non-linear part, which depends on the particle velocity through the slit. The linear resistance R_{sa} can be obtained using [4]:

$$R_{sa} = \frac{12\,\eta\,l}{2\,\pi\,R\,t^3} \tag{7}$$

wherein $\eta = 18.6 \cdot 10^{-6}\,\mathrm{Ns/m^2}$ is the dynamic viscosity of air, l the slit length, $2\pi R$ the slit circumference and t the slit width.

To obtain the velocity dependent part, the loss of kinetic energy of the flow will be considered [5, 6]. Figure 9 shows the situation. During the time span $\mathrm{d}\,\tau$, before entering the slit, the mass $\rho\,S\,u_s\,\mathrm{d}\,\tau$ has

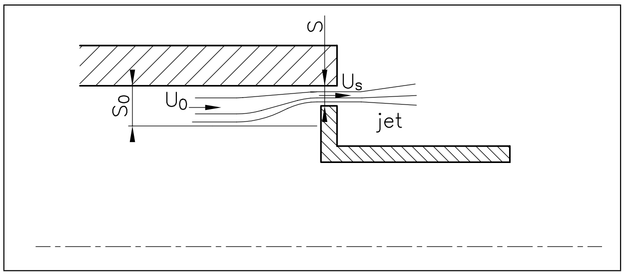

Figure 9. Contraction of the flow through the slit.

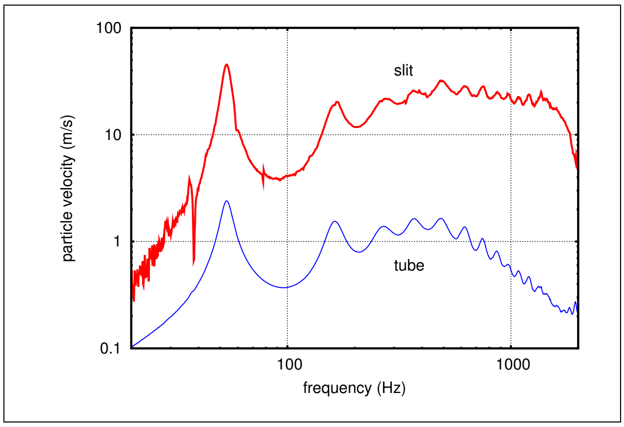

Figure 10. Particle velocity u_0 before the slit (thin blue line) and u_s through the slit (thick red line) while contracting from the surface S_0 to S with a loudspeaker excitation level of 100V.

a velocity u_0 and flows through an area S_0 which is larger than the slit cross-section S. When this mass has to flow through the slit, is has to contract from the surface S_0 to $S = 2\,\pi\,R\,t$ of the slit and the mass accelerates until it reaches the velocity u_s. This is demonstrated by the measurement displayed in figure 10, where the slit velocity (thick red line) increases until 15 times the incoming particle velocity u_0 (thin blue line) due to the surface contraction from S_0 to S. When this mass exits the slit at the other side, a jet will be formed due to the sudden area jump and the kinetic energy of the mass will be dissipated. When the flow alternates, this process happens at both sides of the slit. Although the geometric situation is different at both sides of the slit, it is assumed that the process is the same at both sides. For alternating flow, the difference in kinetic energy W of the mass $\rho\,S\,u_s\,\mathrm{d}\,\tau$ moving through the slit compared to before entering the slit, expressed for a half period T, will be:

$$W = \int_0^{T/2} \rho\,S\,u_s\,\frac{u_s^2 - u_0^2}{2}\,\mathrm{d}\,\tau \tag{8}$$

The kinetic energy W presented in expression (8) is valid when the flow through the slit is uniform. This will be not the case as the Reynolds number:

$$Re = \frac{u_s\,t}{\nu} = \frac{25 \cdot 0.2 \cdot 10^{-3}}{15 \cdot 10^{-6}} = 330 < 2300 \tag{9}$$

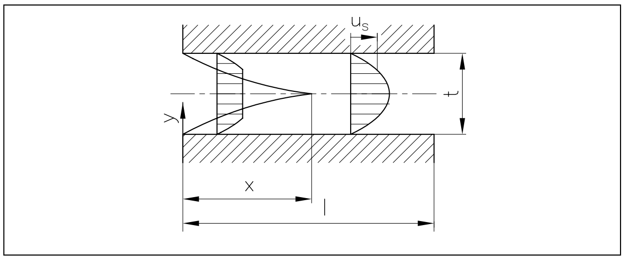

Figure 11. Velocity distribution in the slit during formation of hydrodynamic developed flow.

wherein u_s is the velocity through the slit, obtained from figure 10, $t = 0.2$ mm the slit width and $\nu = 15 \cdot 10^{-6}\,\mathrm{m}^2/\mathrm{s}$ the kinematic viscosity of air. The transition from laminar to turbulent flow takes place when the Reynolds number $Re > 2300$ [7]. The analysis of the Reynolds number points out that the flow in the slit can be laminar. The second condition for laminar flow is that the flow has to be fully hydrodynamically developed. At the entrance of the slit, a shear layer is formed at both sides which agglomerate after a certain travel distance x as presented in figure 11.

This distance x will be [7]:

$$x = Re\, t\, 0.011 = 330 \cdot 0.2 \cdot 0.011 = 0.7\,\mathrm{mm} \quad (10)$$

which is smaller than the slit length $l = 1.5$ mm. Consequently, the slit velocity u will be parabolically distributed over the slit height coordinate y as $u(y) = \frac{3}{2}\,(1 - \frac{y^2}{(t/2)^2})\,u_s$. Introducing this parabolic velocity distribution in expression (8) results in:

$$W = \int_0^{T/2} \rho\, 2\,\pi\, R \int_{-\frac{t}{2}}^{\frac{t}{2}} \frac{u(y)^3 - u_0^2\, u(y)}{2} \mathrm{d}\,y\,\mathrm{d}\,\tau \quad (11)$$

wherein $2\,\pi\,R$ is the slit circumference. The evaluation of the inner integral of the velocity distribution results in:

$$W = \int_0^{T/2} \rho 2\pi R \frac{t}{2} u_s (\alpha u_s^2 - u_0^2) \mathrm{d}\,\tau \text{ with } \alpha = \frac{54}{16} \quad (12)$$

wherein α is a collection of constants resulting from the integration operations.

The volume velocity before the slit and in the slit will be equal, so $\Phi = u_0\, S_0 = u_s\, S$. The surface ratio, which is also called the contraction ratio, between the cross-section which the flow passes through before the slit and the cross-section of the slit itself is $\sigma = \frac{S}{S_0} = \frac{u_0}{u_s}$. Substituting u_0 by $\sigma\, u_s$ in equation (12) results in:

$$W = \int_0^{T/2} \frac{1}{2}\,\rho\, S\, u_s^3\, (\alpha - \sigma^2)\,\mathrm{d}\,\tau \quad (13)$$

wherein $2\,\pi\,R$ is the slit circumference.

In case of harmonic excitation, i.e. $u_0 = u\,\sin\omega t$, the velocity through the slit will be $u_s = \frac{u\,\sin\omega t}{\sigma}$. The integral will be evaluated for a half period of the sine wave, resulting in:

$$W = \frac{2}{3\,\omega}\,\rho\, S\, \frac{\alpha - \sigma^2}{\sigma^3}\, u^3 \quad (14)$$

In analogy to electrical engineering, the resistance R_{su} will be determined from the dissipation energy:

$$W = \int_0^{T/2} R_{su}\, \Phi^2\, \mathrm{d}\,\tau = \int_0^{T/2} R_{su}\, S^2\, u_s^2\, \mathrm{d}\,\tau \quad (15)$$

Replacing u_s by $\frac{u\,\sin\omega t}{\sigma}$ and evaluating the integral (15) results in:

$$W = R_{su}\, \frac{\pi}{2\,\omega}\, S^2\, \frac{u^2}{\sigma^2} \quad (16)$$

The non-linear part of the slit resistance R_{su} will result by comparing expression (16) with (14):

$$R_{su} = \frac{4}{3\,\pi}\, \frac{\rho}{S}\, \frac{\alpha - \sigma^2}{\sigma}\, u \quad (17)$$

The total resistance of the slit is the sum of the linear part (7) and the non-linear part (17):

$$R_s = \frac{12\,\eta\, l}{2\,\pi\, R\, t^3} + \frac{4}{3\,\pi}\, \frac{\rho}{S}\, \frac{\alpha - \sigma^2}{\sigma}\, u \quad (18)$$

The numerical values for the geometry and viscosity are substituted in equation (18). The cross-section ratio $\sigma = 0.067$ is deduced from the particle velocities from figure 10. The result is plotted over the measured resistances in figure 7 in thin blue line. The lower line is simulated for a slit of 0.22 mm width and the upper line for 0.20 mm width. The viscous part of the slit resistance is very sensitive to small variations of the slit width. The measured slit resistances are situated between the two calculated lines. From expression (18), the non-linear part of the slit resistance appears to be proportional to the particle velocity u and independent of frequency. The analysis provides a good estimation of the measured values.

6. Mean flow effects.

The effects of a mean flow on the acoustic damping are investigated by introducing a mean flow in the impedance tube. The mean flow is introduced uniformly around the duct circumference at the loudspeaker end, such that a developed uniform flow is present in the measurement section and the annular tailpipe. The flow volume velocity is measured by a Ritter volumetric gas meter. The flow velocity has been taken into account in the device impedance calculation by introducing the Mach number in the wave number k and in the characteristic duct impedance Z_0 according to Munjal [2].

The resistance of the slit has been measured with a loudspeaker voltage of 20V for different mean flow

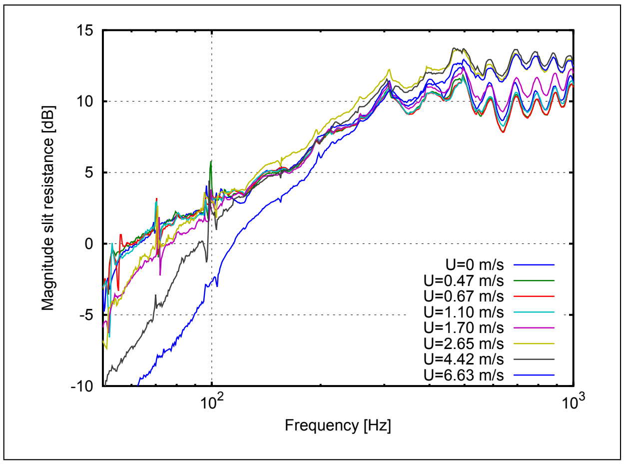

Figure 12. Slit resistance in terms of particle velocity through the slit for different frequencies (thick red lines: measured, thin blue lines: simulated using expression (18))

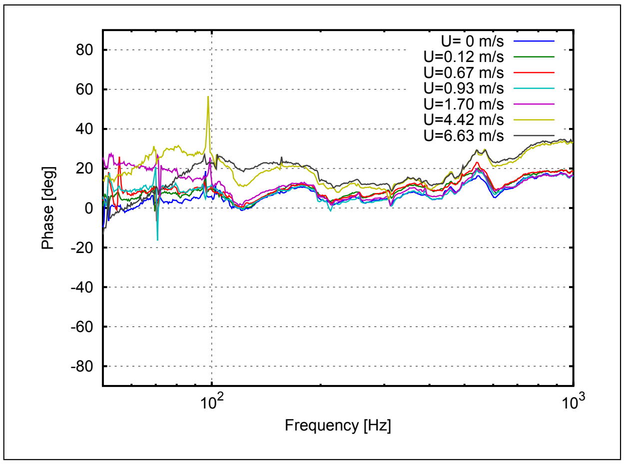

Figure 13. Slit resistance in terms of particle velocity through the slit for different frequencies (thick red lines: measured, thin blue lines: simulated using expression (18))

velocities ranging from 0 to 6.63 m/s in the duct cross-section. The transition from laminar to turbulent flow in the duct situates around the velocity $u <$ 0.9-1.6 m/s.

Figure 12 presents the slit resistance magnitude in terms of frequency for the different flow velocities. The effect of laminar flow on the resistance is barely noticeable. When the flow becomes turbulent, which happens when the flow velocity exceeds 0.9-1.6 m/s, the resistance drops at low frequencies, however, at high frequencies, the resistance tends to the still-standing medium resistance.

Figure 13 presents the phase of the slit resistance. The phase remains around zero degrees which indicates its resistive nature. For turbulent flow, the phase tends to 20 degrees, which still is mainly resistive. The effects of the presence of a mean flow are rather small and the damping mechanism of the slit remains intact.

7. CONCLUSIONS

A damping device, consisting of a central tube surrounded by a narrow slit, has been investigated. It has a neglectable flow resistance. The impedance of the acoustic mass of the central tube increases with frequency, while the slit resistance remains approximately constant in terms of frequency. At higher frequencies, a considerable part of the acoustic flow passes through the slit, where it will be damped. The damping mechanism is two fold: a linear part of the slit resistance in which the viscosity of the air is involved and a non-linear part wherein the slit resistance is proportional to the particle velocity of the air through the slit. In this part, the loss of kinetic energy of the pulsing flow due the abrupt cross-section jumps before and after the slit causes additional flow induced damping. The effects of the presence of a mean flow are rather small and the acoustic damping mechanism of the slit remains intact.

Ultimately, this research will result in development rules for such devices and to optimize the geometry of the annular tube for specific applications.

Acknowledgement

The author thanks the F.W.O. (Fonds Wetenschappelijk Onderzoek) for funding this research project G.0351.09N.

References

[1] R. Boonen, P. Sas, W. Desmet, W. Lauriks, G.Vermeir: Calibration of the two microphone transfer function method with hard wall impedance measurements at different reference sections, Journal of the Mechanical Systems and Signal Processing, Vol. 23, No. 5, (2009), pp. 1662-1671.

[2] M. Munjal: Acoustics of ducts and mufflers with application to exhaust and ventilation system design, John Wiley and sons, (1986)

[3] ISO 10534: Determination of sound absorption coefficient and impedance in impedance tubes, International Organisation for Standardization, Case postale 56, CH-1211 Genève 20, (1998).

[4] L. L. Beranek: Acoustics, Mc Graw-Hill, (1954)

[5] L. J. Sivian: Acoustic impedance of small orifices, Journal of the Acoustical Society of America, Vol. 7, (1935), pp. 94-101.

[6] U. Ingard, S. Labate: Acoustic circulation effects and the nonlinear impedance of orifices, Journal of the Acoustical Society of America, Vol. 22, No. 2, (1949), pp. 211-218

[7] S. Kakac, R. Shah, W. Aung: Handbook of single-phase convective heat transfer, John Wiley & Sons, (1987)